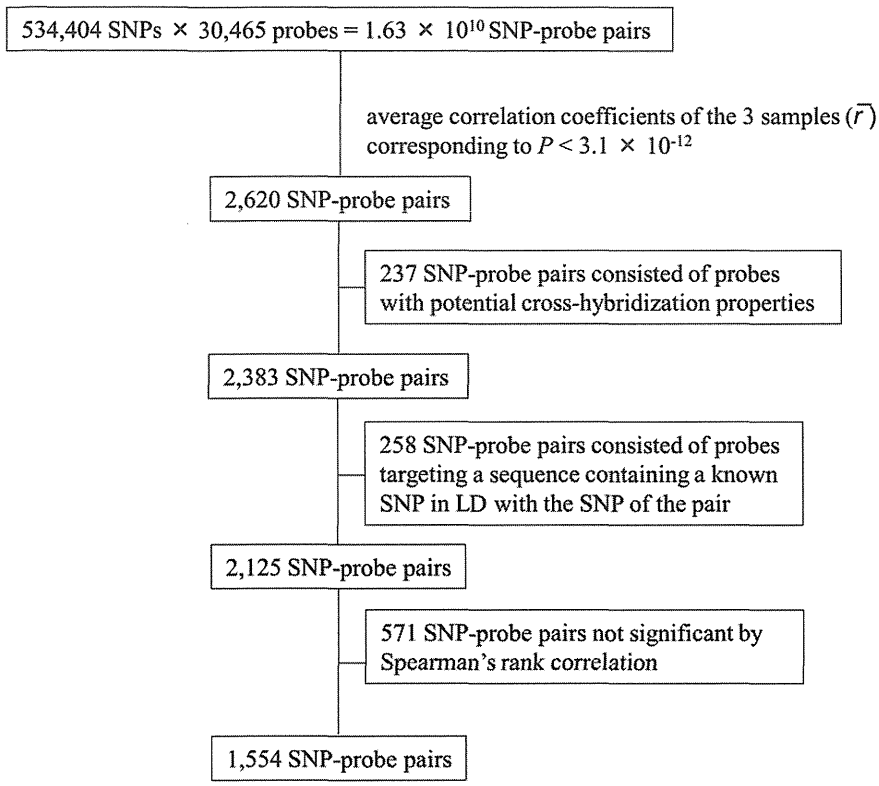

Figure 1. Procedure for selecting significant SNP-probe pairs. The procedure for selecting significant SNP-probe pairs is shown. SNP-probe pairs with a high likelihood of cross-hybridization and SNP-in-probe effects were excluded to exclude false positive results. The SNPs of the remaining 1,554 SNP-probe pairs were considered as eQTL SNPs.
doi:10.1371/journal.pone.0054967.g001

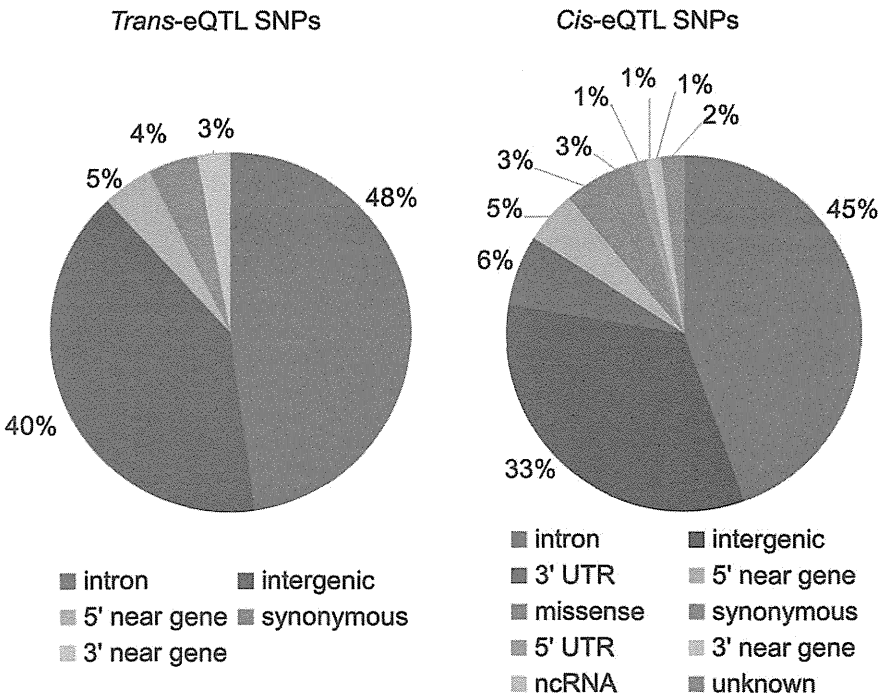

Figure 2. Functional types of the eQTL SNPs. The percentage of SNP types is shown for *cis*- and *trans*- eQTL SNPs.
doi:10.1371/journal.pone.0054967.g002

Since several of the probes targeted the same gene, the total number of genes identified was 107. As shown in Figure 2, the majority of the eQTL SNPs were located in intronic (45% and 48% for *cis*- and *trans*-eQTL SNPs, respectively) or intergenic (33% and 40% for *cis*- and *trans*-eQTL SNPs, respectively) regions.

Table S2 shows the names and properties of the 107 genes whose expression levels in whole blood were affected by SNPs. The SNPs affecting expression levels of the same gene were primarily in high LD with each other. Furthermore, investigation of combined Chinese and Japanese (CHB+JPT) panels from the 1000 Genomes Pilot 1 SNP data set and the HapMap release 22 data set showed a greater number of SNPs in high LD ($r^2>0.8$) with the eQTL SNPs identified in the current study. Since the high intermarker correlations cause difficulties in determining which SNP is responsible for the regulation of gene expression, we defined the eQTL region of a gene as the genomic range in which the SNPs in LD ($r^2>0.8$) with the eQTL SNPs of the gene are located. LD was determined by SNAP [20] using the population panel CHB+JPT from the 1000 Genomes Pilot 1 SNP data set and the HapMap release 22 data set.

Locational Relationships between the eQTL and the Gene

Regarding the locational relationships between the eQTL and the gene, 102 of the eQTLs were *cis*-acting (within 1 Mb upstream or downstream of the gene), and 5 were *trans*-acting, of which 4 were located on a different chromosome from the gene that they influenced. When the genome was divided into 3 segments (i.e., upstream, intragenic, and downstream), 69 *cis*-acting eQTL regions covered multiple segments that included the intragenic segments, 13 were confined to upstream segments, 7 were confined to downstream segments, and 13 were confined to intragenic segments.

Comparison of Results with Previously Reported Whole Blood eQTLs

We compared our results with those of the study by Fehrmann et al. [21], which performed a genome-wide eQTL analysis on 289,044 SNPs in whole blood expression data of 1,469 unrelated individuals from the United Kingdom and the Netherlands. The genotyping platform which they used (Illumina HumanHap300 platform) included only 24% of the 534,404 SNPs analyzed in the current study and 15% of the 1,153 eQTL SNPs identified in the current study. Therefore, 85% of the eQTL SNPs identified in the current study had not been identified by Fehrmann et al. [21], because they were not included in the Illumina HumanHap300 platform. On the other hand, 84% of the eQTL SNPs identified in the current study which were included in the Illumina HumanHap300 platform had also been identified as eQTL SNPs in their study. The high replication rate supports the robustness of our findings.

Influence on Expression Levels in Lymphoblastoid Cell Lines

Next, we examined whether the eQTL SNPs affecting the expression levels in whole blood also influence expression levels in lymphoblastoid cell lines. We selected representative SNPs in eQTL regions and examined their effects on the expression of the corresponding gene in lymphoblastoid cell lines. The SNPs that showed the strongest correlation with the expression levels in whole blood for each eQTL region were selected for examination of the possible effects on expression levels in lymphoblastoid cell lines. If there were any additional eQTL SNPs in the same region that were not in LD with the selected SNP ($r^2<0.1$), then one of the SNPs with the strongest correlation with the expression levels in whole blood was also selected. In the eQTL regions for *MICA*, *MICB*, *HLA-DRB5*, *HLA-DQB1*, and *HLA-DQA2*, 2 representative SNPs, which were not in significant LD with each other ($r^2<0.1$), were selected. For other genes, the eQTL SNPs in the same eQTL region were in LD with each other ($r^2>0.1$); therefore, 1 representative SNP was selected for each region. If the genotype data of the selected SNP were not available in the HapMap data, the SNP within the same eQTL region having the next strongest correlation with the expression levels in whole blood was selected.

Genotype and expression levels in lymphoblastoid cell lines were retrieved from public data for 45 Japanese individuals for 88 (86 *cis* and 2 *trans*) of the 112 representative SNPs. The average number of individuals with applicable data for genotype and the expression levels of lymphoblastoid cell lines in the 88 retrieved SNP-gene pairs was 43.8. The Pearson's correlation coefficients between the eQTL SNPs and the expression levels of the corresponding genes in lymphoblastoid cell lines were calculated and have been shown in Table S3. A positive correlation coefficient indicates that the SNP has a similar effect on expression levels in whole blood and lymphoblastoid cell lines. Of the 86 *cis*-eQTL SNPs, 34 showed a significantly positive correlation, whereas 13 showed a significantly negative correlation with the expression levels of lymphoblastoid cell lines (FDR-corrected, $P<0.05$). None of the *trans*-eQTL SNPs identified in the current study significantly affected expression levels in lymphoblastoid cell lines.

Functional Properties of the eQTL SNPs

We examined whether the regulatory effects of eQTL SNPs were caused by mutations in transcription factor-binding sites (TFBSs), splicing-affecting sites, or microRNA (miRNA)-binding sites. The proportion of SNPs in LD ($r^2>0.8$) with a SNP predicted to be located on such sites was compared between the 37 eQTL SNPs affecting expression levels in both whole blood and lymphoblastoid cell lines; 49 eQTL SNPs affecting only whole blood expression levels; and 5,681 non-eQTL SNPs located within 100 kB of the 107 genes that were regulated by the eQTL SNPs identified in the current study. A web-based tool (FuncPred; http://snpinfo.niehs.nih.gov/snpinfo/snpfunc.htm) was used to predict the functional properties of the SNPs. As shown in Table 1, eQTL SNPs were more likely to be in LD with SNPs located on TFBSs, splicing-affecting sites, and miRNA-binding sites.

Cis-only Analysis

The small-effect eQTL SNPs are likely to have remained undetected in the present study due to the strict correction procedures for multiple testing. In order to reduce the number of unreported *cis*-eQTL SNPs, we also performed *cis*-only analysis by examining only SNPs 1 Mb upstream or downstream of the targeted gene. A total of 955,370 SNP-probe pairs were examined, and those with an average Pearson's correlation ($\bar{r}$) of the 3 sample groups corresponding to $P<5.23\times10^{-9}$ (i.e., Bonferroni-corrected $P<0.05$) were considered significant. As shown in Table S4, the *cis*-only analysis resulted in 3,883 SNP-probe pairs consisting of 3,161 SNPs and 347 probes.

The Influence of Depressive Disorder on Gene Expression Regulation

In order to investigate whether depressive disorder was a major confounding factor for gene expression regulation, we calculated the Spearman's correlation coefficients separately in depressed and non-depressed subjects. All the 1,554 SNP-probe pairs identified

Table 1. Percentage of SNPs that are in linkage disequilibrium ($r^2>0.8$) with a SNP predicted to be located on TFBS, splicing-affecting site, or miRNA binding site.

	TFBS	Splicing	miRNA binding site
eQTL SNPs affecting expression levels in both whole blood and LCLs (37 SNPs)	73.7% ‡	42.1% ‡	44.7% ‡
eQTL SNPs affecting expression levels in only whole blood (49 SNPs)	58.8% ‡	43.1%‡	29.4% †
non-eQTL SNPs (5,681 SNPs)	34.8%	17.3%	14.1%

The following abbreviations are used: TFBS, transcription factor binding site; miRNA, micro RNA; LCL, lymphoblastoid cell line.
†$P<0.01$,
‡$P<0.001$: Significantly higher compared to non-eQTL SNPs (χ^2 test).
doi:10.1371/journal.pone.0054967.t001

as eQTL in the present study achieved high correlations for both depressed and non-depressed subjects (average Spearman's correlation of the 3 sample groups $\overline{\rho}>0.4$, FDR-corrected $P<0.01$ in non-depressed subjects and $\overline{\rho}>0.5$, FDR-corrected $P<0.005$ in depressed subjects for all 1,554 SNP-probe pairs).

Discussion

To our knowledge, this is the first genome-wide eQTL study in Asian subjects that examined the association of SNPs with expression levels in whole blood. The genome-wide investigation uncovered 1,153 SNPs affecting gene expression levels in human whole blood. Although the number of eQTL regions identified in the current study was relatively small, the likelihood of false positives is low because of the strict correction procedures for multiple testing and exclusion of SNPs with potential cross-hybridization or SNP-in-probe effects.

Since SNPs in strong LD with a SNP directly responsible for regulating gene expression levels are also correlated with gene expression levels, it is difficult to determine which SNP is the causative one. We assumed that the genetic regulatory locus would be included in the eQTL region, defined as the genomic range in which the SNPs in LD ($r^2>0.8$) with the eQTL SNPs identified in our study are found. Although the numerous SNPs in LD with each other hindered the identification of the responsible SNP, the locations of the eQTL regions indicated that eQTLs are widely distributed both upstream and downstream of the gene, as well as within the gene.

The current study showed that several of the SNPs affecting the expression levels of a gene in whole blood also influenced the expression levels of the same gene in lymphoblastoid cell lines. A recent study by Powell et al. [22] has shown that the genetic control mechanisms of gene expression in whole blood and lymphoblastoid cell lines are largely independent. Despite the evidence of low genetic correlation of regulatory variation averaged across the genome, our results suggest that a subset of eQTLs commonly affect expression levels in whole blood and lymphoblastoid cell lines. Conversely, our findings suggest that some of the whole blood eQTL SNPs do not regulate expression levels in lymphoblastoid cell lines. This is in line with a previous study that reported that 69–80% of the identified regulatory variants operated in a cell type-specific manner [9]. Compared to SNPs affecting only expression levels in whole blood, higher, although not statistically significant, proportion of SNPs affecting expression levels in both whole blood and lymphoblastoid cell lines were in LD with SNPs located on TFBSs and miRNA-binding sites. The finding suggests that these functional properties affect expression levels across multiple cell types.

Intriguingly, 13 of the 88 eQTL SNPs in whole blood were observed to have opposite effects on expression levels in whole blood and lymphoblastoid cell lines. Dimas et al. [9] compared gene expression variation in fibroblasts, lymphoblastoid cell lines, and T cells and reported that the same directional effect in each cell type was observed for eQTLs shared between multiple cell types. However, 2 recently published studies reported that some eQTL SNPs have opposite allelic effects on gene expression in the liver, adipose tissue, skeletal muscle [10], or in B cells and monocytes [11]. Our findings also suggest the possibility that some SNPs may exert opposite effects on gene expression in different cell types. However, an alternative explanation may be that the eQTL SNPs identified may function to alter the splicing of the mRNA. Since the gene expression microarray platform used in the previous eQTL study examining LCL expression levels in Japanese subjects was different from ours, the different probes may have detected different splicing variants, resulting in seemingly opposite allelic effects. A comparison using the same platform would be necessary to uncover cell-specific effects on expression levels.

The strength of the current study is that a relatively homogeneous Japanese population was used, which may have minimized the effects of differential genetic backgrounds. The major limitation of the current study is that the conservative corrections for multiple testing may have missed a large proportions of eQTL SNPs. Increasing power allows better detection of weaker and more distantly located *cis*-regulatory elements [23]. Greater than 82% of the significant eQTL-probe pairs identified in the current study had $P<3.1\times10^{-13}$, which far exceeded the predetermined significance level ($P<3.1\times10^{-12}$). Our findings should not be generalized to more weakly associated eQTLs since they may have different regulatory mechanisms. Another limitation is that approximately half of the samples were collected from patients with a depressive disorder. However, analyzing healthy and depressive subjects separately also resulted in achieving high correlations (FDR-corrected $P<0.01$) for all the 1,554 SNP-probe pairs identified in the current study. Therefore, it is unlikely that depressive disorder has a major impact on gene expression regulation of the identified eQTL SNPs. Further investigation on the influence of depressive symptoms on gene expression levels is underway using a larger sample size.

In summary, we have presented the results on genome-wide investigations of SNPs affecting the expression levels in whole blood. Both *cis*-acting and *trans*-acting eQTL SNPs were identified for a total of 107 genes. The eQTL regions were widely distributed upstream, downstream, and within the gene sequence. The findings of this study are valuable if gene expression levels in whole blood are used as biomarkers for disease conditions. Gene expression levels and their connection with disease-associated SNPs may lead to a better understanding of genetic predisposition to disease and may be used to predict disease susceptibility. Further studies are required to clarify how SNPs function in

affecting the expression levels in whole blood as well as in other tissues.

Supporting Information

Table S1 Significant SNP-probe pairs. The SNP-probe pair selection procedure generated 1,554 significant pairs, consisted of 1,153 SNPs, defined as eQTL SNPs, and 185 probes.
(XLSX)

Table S2 Genes whose expression levels in whole blood are affected by SNPs. The names and properties of the 107 genes whose expression levels in whole blood were affected by SNPs are shown.
(XLSX)

Table S3 The Pearson's correlation coefficients between the eQTL SNPs and the expression levels of the corresponding genes in lymphoblastoid cell lines. A positive correlation coefficient indicates that the SNP has a similar effect on expression levels in whole blood and lymphoblastoid cell lines. Of the 86 *cis*-eQTL SNPs, 34 showed a significantly positive correlation, whereas 13 showed a significantly negative correlation with the expression levels of lymphoblastoid cell lines (FDR-corrected, $P<0.05$).
(XLSX)

Table S4 The results of the *cis*-only analysis. The *cis*-only analysis resulted in 3,883 SNP-probe pairs consisting of 3,161 SNPs and 347 probes.
(XLSX)

Acknowledgments

The authors would like to thank the participants for taking part in the study.

Author Contributions

Conceived and designed the experiments: DS HH HK. Performed the experiments: DS SN RM NY. Analyzed the data: DS HH SN RM TT KH MO. Contributed reagents/materials/analysis tools: DS HH TT KH MO NY HK. Wrote the paper: DS TH NA HK.

References

1. Emilsson V, Thorleifsson G, Zhang B, Leonardson AS, Zink F, et al. (2008) Genetics of gene expression and its effect on disease. Nature 452: 423–428.
2. Mehta D, Heim K, Herder C, Carstensen M, Eckstein G, et al. (2012) Impact of common regulatory single-nucleotide variants on gene expression profiles in whole blood. Eur J Hum Genet.
3. Goring HH, Curran JE, Johnson MP, Dyer TD, Charlesworth J, et al. (2007) Discovery of expression QTLs using large-scale transcriptional profiling in human lymphocytes. Nat Genet 39: 1208–1216.
4. Innocenti F, Cooper GM, Stanaway IB, Gamazon ER, Smith JD, et al. (2011) Identification, replication, and functional fine-mapping of expression quantitative trait loci in primary human liver tissue. PLoS Genet 7: e1002078.
5. Stranger BE, Forrest MS, Clark AG, Minichiello MJ, Deutsch S, et al. (2005) Genome-wide associations of gene expression variation in humans. PLoS Genet 1: e78.
6. Veyrieras JB, Kudaravalli S, Kim SY, Dermitzakis ET, Gilad Y, et al. (2008) High-resolution mapping of expression-QTLs yields insight into human gene regulation. PLoS Genet 4: e1000214.
7. Holm K, Melum E, Franke A, Karlsen TH (2010) SNPexp - A web tool for calculating and visualizing correlation between HapMap genotypes and gene expression levels. BMC Bioinformatics 11: 600.
8. Yang TP, Beazley C, Montgomery SB, Dimas AS, Gutierrez-Arcelus M, et al. (2010) Genevar: a database and Java application for the analysis and visualization of SNP-gene associations in eQTL studies. Bioinformatics 26: 2474–2476.
9. Dimas AS, Deutsch S, Stranger BE, Montgomery SB, Borel C, et al. (2009) Common regulatory variation impacts gene expression in a cell type-dependent manner. Science 325: 1246–1250.
10. Fu J, Wolfs MG, Deelen P, Westra HJ, Fehrmann RS, et al. (2012) Unraveling the regulatory mechanisms underlying tissue-dependent genetic variation of gene expression. PLoS Genet 8: e1002431.
11. Fairfax BP, Makino S, Radhakrishnan J, Plant K, Leslie S, et al. (2012) Genetics of gene expression in primary immune cells identifies cell type-specific master regulators and roles of HLA alleles. Nat Genet 44: 502–510.
12. Ding J, Gudjonsson JE, Liang L, Stuart PE, Li Y, et al. (2010) Gene expression in skin and lymphoblastoid cells: Refined statistical method reveals extensive overlap in cis-eQTL signals. Am J Hum Genet 87: 779–789.
13. Whitney AR, Diehn M, Popper SJ, Alizadeh AA, Boldrick JC, et al. (2003) Individuality and variation in gene expression patterns in human blood. Proc Natl Acad Sci U S A 100: 1896–1901.
14. Alberts R, Terpstra P, Li Y, Breitling R, Nap JP, et al. (2007) Sequence polymorphisms cause many false cis eQTLs. PLoS One 2: e622.
15. Stranger BE, Forrest MS, Dunning M, Ingle CE, Beazley C, et al. (2007) Relative impact of nucleotide and copy number variation on gene expression phenotypes. Science 315: 848–853.
16. Berisha SZ, Serre D, Schauer P, Kashyap SR, Smith JD (2011) Changes in whole blood gene expression in obese subjects with type 2 diabetes following bariatric surgery: a pilot study. PLoS One 6: e16729.
17. Taurines R, Grunblatt E, Schecklmann M, Schwenck C, Albantakis L, et al. (2011) Altered mRNA expression of monoaminergic candidate genes in the blood of children with attention deficit hyperactivity disorder and autism spectrum disorder. World J Biol Psychiatry 12 Suppl 1: 104–108.
18. Purcell S, Neale B, Todd-Brown K, Thomas L, Ferreira MA, et al. (2007) PLINK: a tool set for whole-genome association and population-based linkage analyses. Am J Hum Genet 81: 559–575.
19. Faller AJ (1981) An Average Correlation Coefficient. Journal of Applied Metereology 20: 203–205.
20. Johnson AD, Handsaker RE, Pulit SL, Nizzari MM, O'Donnell CJ, et al. (2008) SNAP: a web-based tool for identification and annotation of proxy SNPs using HapMap. Bioinformatics 24: 2938–2939.
21. Fehrmann RS, Jansen RC, Veldink JH, Westra HJ, Arends D, et al. (2011) Trans-eQTLs reveal that independent genetic variants associated with a complex phenotype converge on intermediate genes, with a major role for the HLA. PLoS Genet 7: e1002197.
22. Powell JE, Henders AK, McRae AF, Wright MJ, Martin NG, et al. (2012) Genetic control of gene expression in whole blood and lymphoblastoid cell lines is largely independent. Genome Res 22: 456–466.
23. Dobrin R, Greenawalt DM, Hu G, Kemp DM, Kaplan LM, et al. (2011) Dissecting cis regulation of gene expression in human metabolic tissues. PLoS One 6: e23480.

Biochemical and Biophysical Research Communications 433 (2013) 450–455

Contents lists available at SciVerse ScienceDirect

Biochemical and Biophysical Research Communications

journal homepage: www.elsevier.com/locate/ybbrc

Gene expression levels of S100 protein family in blood cells are associated with insulin resistance and inflammation (Peripheral blood S100 mRNAs and metabolic syndrome)

Masaya Yamaoka [a], Norikazu Maeda [a,*], Seiji Nakamura [b], Takuya Mori [a], Kana Inoue [a], Keisuke Matsuda [a], Ryohei Sekimoto [a], Susumu Kashine [a], Yasuhiko Nakagawa [a], Yu Tsushima [a], Yuya Fujishima [a], Noriyuki Komura [a], Ayumu Hirata [a], Hitoshi Nishizawa [a], Yuji Matsuzawa [c], Ken-ichi Matsubara [b], Tohru Funahashi [a,d], Iichiro Shimomura [a]

[a] Department of Metabolic Medicine, Graduate School of Medicine, Osaka University, 2-2-B5 Yamada-oka, Suita, Osaka 565-0871, Japan
[b] DNA Chip Research Inc., 1-1-43, Suehiro-cho, Tsurumi-ku, Yokohama, Kanagawa 230-0045, Japan
[c] Sumitomo Hospital, 5-3-20, Nakanoshima, Kita-ku, Osaka, Osaka 530-0005, Japan
[d] Department of Metabolism and Atherosclerosis, Graduate School of Medicine, Osaka University, 2-2-B5 Yamada-oka, Suita, Osaka 565-0871, Japan

ARTICLE INFO

Article history:
Received 25 February 2013
Available online 15 March 2013

Keywords:
Obesity
Metabolic syndrome
Inflammation
S100 family
Insulin resistance

ABSTRACT

Objective: Visceral fat obesity is located upstream of metabolic syndrome and atherosclerotic diseases. Accumulating evidences indicate that several immunocytes including macrophages infiltrate into adipose tissue and induce chronic low-grade inflammation. We recently analyzed the association between visceral fat adiposity and the gene expression profile in peripheral blood cells in human subjects and demonstrated the close relationship of visceral fat adiposity and disturbance of circadian rhythm in peripheral blood cells. In a series of studies, we herein investigated the association of visceral fat adiposity and mRNA levels relating to inflammatory genes in peripheral blood cells.

Approach and Results: Microarray analysis was performed in peripheral blood cells from 28 obese subjects. Reverse transcription-polymerase chain reaction (RT-PCR) was conducted by using blood cells from 57 obese subjects. Obesity was defined as body mass index (BMI) greater than 25 kg/m^2 according to the Japanese criteria. Gene expression profile analysis was carried out with Agilent whole human genome 4 × 44 K oligo-DNA microarray. Gene ontology (GO) analysis showed that 14 genes were significantly associated with visceral fat adiposity among 239 genes relating to inflammation. Among 14 genes, RT-PCR demonstrated that S100A8, S100A9, and S100A12 positively correlated with visceral fat adiposity in 57 subjects. Stepwise multiple regression analysis showed that S100A8 and S100A12 mRNA levels were closely associated with HOMA-IR and S100A9 mRNA was significantly related to adiponectin and CRP.

Conclusions: Peripheral blood mRNA levels of S100 family were closely associated with insulin resistance and inflammation.

1. Introduction

Obesity, especially visceral fat-accumulated obesity, is closely associated with the development of atherosclerotic diseases and is strongly linked to metabolic syndrome [1]. Molecular mechanism for metabolic syndrome has been investigated but it has not been fully understood at present. Increasing evidences indicate that several immunocytes including macrophages infiltrate into adipose tissue and induce chronic low-grade inflammation, which develops into insulin resistance and metabolic syndrome [2]. Moreover, these immune cells interact with adipocytes through free fatty acids and adipocytokines, generating a vicious metabolic cycle that accelerates the development of metabolic syndrome and atherosclerosis [3,4].

These pathologies in obese fat tissue suggest that gene expression profile in peripheral blood cells may reflect the visceral fat condition. Recently, we examined and analyzed the association between visceral fat adiposity and the gene expression profile in peripheral blood cells to search novel surrogate markers relating to visceral fat adiposity and to establish novel diagnostic tools for metabolic syndrome [5]. Interestingly, genes relating to circadian rhythm were significantly correlated with visceral fat adiposity, suggesting that visceral fat adiposity links to disturbance of

* Corresponding author. Fax: +81 6 6879 3739.
E-mail address: norikazu_maeda@endmet.med.osaka-u.ac.jp (N. Maeda).

0006-291X/$ - see front matter © 2013 Elsevier Inc. All rights reserved.
http://dx.doi.org/10.1016/j.bbrc.2013.02.096

circadian rhythm. In a series of studies for the impact of visceral fat adiposity on the gene expression profile in peripheral blood cells, we here analyzed the association of visceral fat adiposity and expression levels of inflammatory genes in peripheral blood cells.

2. Methods

2.1. Study population and clinical examinations

All subjects were inpatients of the Division of Endocrinology & Metabolism, Osaka University Hospital, Osaka, Japan. Written informed consent was obtained from each subject after explaining the purpose and potential complications of the study. The study protocol was approved by the human ethics committee of Osaka University and the study was registered with the University hospital Medical Information Network (Number: UMIN 000001663). Subjects and clinical examinations were described previously. Patients with type 1 diabetes mellitus, autoimmune diseases, malignant diseases, and infectious diseases were excluded from the study. Patients treated with statin and/or thiazolidinediones were also excluded. The estimated visceral fat area (eVFA) was measured by abdominal bioelectrical impedance analysis (BIA), as reported previously [6,7]. The homeostasis model-assessment of insulin resistance (HOMA-IR) was calculated by the equation: HOMA-IR = fasting insulin (μU/mL) × fasting glucose (mg/dL)/405.

2.2. Microarray analysis

Blood samples were collected into PaxGene Blood RNA tubes (PreAnalytiX/QIAGEN Inc., Valencia, CA) at 7:30 am. Total RNA was extracted by using PaxGene Blood RNA Kit (PreAnalytiX/QIAGEN) according to the protocol supplied by the manufacturer. After RNAs were qualified by the Agilent 2100 Bioanalyzer, total RNA was converted to cDNA, amplified, and labeled with Cy3-labeled CTP using the Quick Amp Labeling kit (Agilent Technologies, Santa Clara, CA). The amplified RNA and dye incorporation were quantified using a ND-1000 Spectrophotometer (Nano Drop Technologies, Wilmington, DE) and hybridized to Agilent whole human genome 4 × 44 K oligo-DNA microarray (Agilent Technologies, Santa Clara, CA). After hybridization, the arrays were washed consecutively by using Gene Expression Wash Pack (Agilent Technologies). Fluorescence images of the hybridized arrays were generated using the Agilent DNA Microarray Scanner, and the intensities were extracted with Agilent Feature Extraction software ver.10.7.3.1. The raw microarray data are deposited in the National Center for Biotechnology Information Gene Expression Omnibus (GEO Series GSE28038).

2.3. Real-time RT-PCR

First-strand cDNA was synthesized from 180 ng of total RNA using Thermoscript RT (Invitrogen, Carlsbad, CA) and oligo dT primer. Real-time quantitative PCR amplification was performed with the LightCycler 1.5 (Roche Diagnostics, Tokyo, Japan) using LightCycler-FastStart DNA Master SYBR Green I (Roche Diagnostics, Tokyo, Japan). The final result for each sample was normalized to the respective GAPDH (glyceraldedyde-3-phosphate dehydrogenase) value. The primer sets used were: S100A8, 5′-CATGCCGTCTACAGGGATGA-3′ and 5′-GACGTCTGCACCCTTTTTCC-3′; S100A9, 5′-GGGAATTCAAAGAGCTGGTG-3′ and 5′-CACTGTGATCTTGGCCACTG-3′; S100A12, 5′-GCTCCACATTCCTGTGCATTGAGG-3′ and 5′-CCCTCATTGAGGACATTGCTGGG-3′; GAPDH, 5′-AAGGGCATCCTGGGCTACA-3′ and 5′-GAGGAGTGGGTGTCGCTGTTG-3′.

2.4. Microarray data analyses

The raw microarray intensities were processed by the percentile shift method (75th percentile) using the GeneSpring GX11 (Agilent Technologies) so as to normalize the range of expression intensities for inter-microarray. Only those genes whose expression data were available in more than 50% of hybridizations were included for further analyses. The normalized data were exported from the GeneSpring GX software. The correlation between peripheral blood gene expression levels and Log-eVFA levels was examined by Pearson's correlation under the R environment (http://cran.at.r-project.org). Gene Ontology (GO) information was retrieved from the annotations in GeneSpring GX11.

2.5. Clinical data analysis

Geometric mean values were used for C-reactive protein (CRP) due to the skewed distribution of the data. Non-normally distributed variables were log-transformed before analysis. The Spearman rank correlation coefficients for the study population as a whole were analyzed for Log-eVFA levels and other clinical variables. P values less than 0.05 denoted the presence of significant difference. Pearson's correlation coefficient was used to examine the relationship between S100A8, S100A9 and S100A12 and metabolic parameters. Stepwise multiple regression analysis was conducted to identify those parameters that significantly contributed to S100A8, S100A9 and S100A12, and parameter with F value > 4.0 were subsequently entered into the regression analysis as independent variables. All calculations were performed using the JMP software (JMP 9.0; SAS Institute Inc., Cary, NC). Data are expressed as mean ± SD.

3. Results

3.1. Characteristics of the subjects

The clinical characteristics of the participating subjects are listed in our previous report [5]. Briefly, the mean BMI, eVFA, and HOMA-IR of 57 patients were 30.6 kg/m^2, 168.8 cm^2, and 3.0, respectively. The proportion of patients with diabetes mellitus, dyslipidemia, and hypertension was 73%, 75%, and 58%, respectively. These clinical characteristics indicate that present study population is typical obesity with multiple complications.

3.2. Analysis of gene expression profiles

Microarray analysis was performed by using peripheral blood RNA samples from 28 subjects (BMI 31.9 ± 6.0 kg/m^2, VFA 199.4 ± 89.4 cm^2). The target probes were selected under the condition that significant signals were detected in more than 14 cases and finally 27,969 genes were extracted for gene expression analysis. To examine the correlation of visceral fat adiposity and peripheral blood mRNA expression levels relating to inflammation, genes classified as inflammation by gene ontology were extracted from among genes associated with visceral fat adiposity. Table 1 lists the significant genes related to inflammation (GO:0006954). Significant association was observed in 14 genes among 239 genes (5.9%) relating to inflammation. Nuclear factor related to kappaB binding protein (NFRKB), which belongs to family of eukaryotic transcription factors that control the expression of a large number of genes regulating inflammation and immunity, was most strongly correlated with eVFA (P = 0.0018). Interestingly, 3 genes, S100A12, S100A8, and S100A9, which belong to S100 protein family, emerged as significantly correlated genes with eVFA.

Table 1
Genes relating to inflammation (GO:0006954).

Gene symbol	Gene name	Correlation	*P* value
NFRKB	Nuclear factor related to kappaB binding protein	−0.563	0.0018
S100A12	S100 calcium binding protein A12	0.538	0.0031
ADORA3	Adenosine A3 receptor	−0.536	0.0033
IL15	Interleukin 15	0.524	0.0042
S100A8	S100 calcium binding protein A8	0.468	0.0120
CCL21	Chemokine (C–C motif) ligand 21	0.463	0.0131
S100A9	S100 calcium binding protein A9	0.439	0.0194
BMP6	Bone morphogenetic protein 6	−0.430	0.0224
PROK2	Prokineticin 2	0.428	0.0230
CCR3	Chemokine (C–C motif) receptor 3	−0.412	0.0293
CCR7	Chemokine (C–C motif) receptor 7	−0.411	0.0296
PXK	PX domain containing serine/threonine kinase	0.406	0.0320
LY96	Lymphocyte antigen 96	0.384	0.0434
TLR5	Toll-like receptor 5	0.374	0.0497

RT-PCR was next performed in 57 subjects to revalue the association of eVFA and S100A8, S100A9, and S100A12 in peripheral blood cells. As shown in Fig. 1, S100A8, S100A9 and S100A12 mRNA levels significantly and positively correlated with eVFA (S100A8, $P = 0.018$, $R = 0.31$; S100A9, $P = 0.047$, $R = 0.26$; S100A12; $P = 0.0013$, $R = 0.41$).

3.3. Association between S100 protein family and clinical parameters

Tables 2–4 lists the correlation coefficients for the relationship between S100A8, S100A9, and S100A12 and various clinical parameters, respectively. In age, sex-adjusted simple correlation analysis, S100A8 mRNA level correlated positively with log-eVFA, HOMA-IR, WBC, neurotrophilis, and CRP, while its mRNA level correlated negatively with log-adiponectin (Table 2). S100A9 mRNA level correlated positively with WBC, neurotrophilis, and CRP, whereas its mRNA level correlated negatively with HDL-C and log-adiponectin (Table 3). S100A12 mRNA level correlated positively with BMI, WC, log-VFA, HOMA-IR, and CRP, while its mRNA level correlated negatively with log-adiponectin (Table 4). Finally, stepwise multiple regression analysis was performed. HOMA-IR was identified as significant determinants of S100A8 ($F = 5.10$) and S100A12 ($F = 6.84$) (Table 2 and 4). Log-adiponectin ($F = 6.23$) and CRP ($F = 11.0$) were significant determinants of S100A9 (Table 3).

4. Discussion

In the present study, we show that peripheral blood S100-relating genes were strongly associated with CRP, adiponectin, and HOMA-IR in obese subjects.

Our group for the first time demonstrated that S100A8 is highly expressed in obese adipose tissues and adipose S100A8 is significantly reduced by peroxisome proliferator-activated receptor-γ (PPARγ) agonist, indicating that S100A8 is one of adipocytokines [8]. Furthermore, we recently showed that circulating level of calprotectin (S100A8/A9 complex) is positively correlated with visceral fat area [9] and is associated with low ultrasonographic low carotid plaque density [10]. Several groups have also showed the clinical significance of calprotectin and suggested that calprotectin is a novel biomarker of cardiovascular events [11–13]. Calprotectin is also higher in obese subjects than in non-obese subjects and is decreased by weight reduction [14,15]. Calprotectin promotes ROS generation via NADPH oxidase activation [16], binds to toll-like receptor 4 (TLR4) [17], and associates with the receptor for advanced glycation end-products (RAGE) [18], suggesting that calprotectin accelerates vital signaling pathways involved in the pathogenesis of atherosclerosis. Plasma S100A12 concentration is increased in type 2 diabetes and cardiovascular diseases [19–21]. Interestingly, the overexpression of human S100A12 induced arterial calcification in mice [22], suggesting that S100A12 is associated with the development of atherosclerosis. Collectively, S100A8, S100A9, and S100A12 may take part in the development of atherosclerosis and type 2 diabetes, because of their pro-inflammatory properties.

However, little is known in the association between peripheral blood mRNA expression levels of S100 family and inflammatory diseases in human. In patients with Kawasaki disease, leukocyte mRNA levels of S100A8, S100A9, and S100A12 were increased at acute phase compared to stable phase [23]. S100A12 mRNA level in peripheral blood mononuclear cells (PBMCs) was higher in non-diabetic subjects with pre-mature coronary artery disease than in the subjects with multiple coronary risk factors [24]. In present study, mRNA expression levels of peripheral blood S100A8, S100A9, and S100A12 were significantly correlated with visceral fat area, although its mechanism remains uncertain.

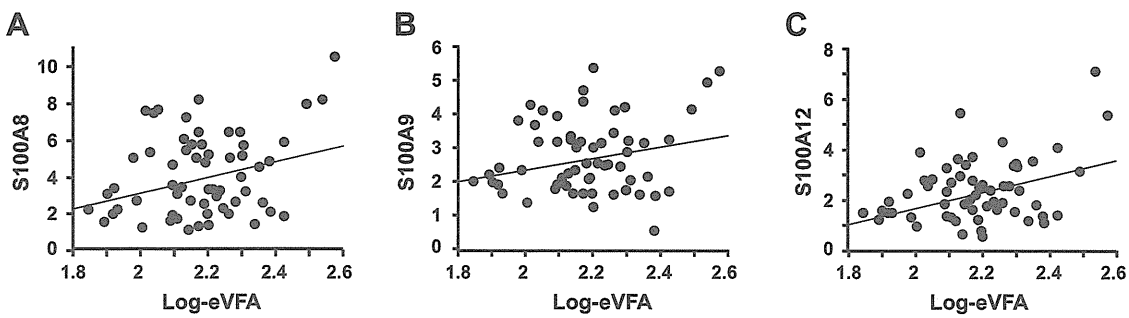

Fig. 1. Correlation of visceral fat area and peripheral blood mRNA levels of S100 family. Total RNAs from peripheral blood cells of 57 subjects were subjected to RT-PCR. S100A8, $P = 0.018$, $R = 0.31$; S100A9, $P = 0.047$, $R = 0.26$; S100A12; $P = 0.0013$, $R = 0.41$.

Table 2
Correlation between peripheral blood S100A8 mRNA and clinical parameters.

Clinical parameters	Univariate (non-adjusted)		Univariate (age, sex-adjusted)		Multivariate	
	R	*P* value	*R*	*P* value	*P* value	*F* value
Age	−0.57	<0.0001	–	–		
Sex	0.19	0.16	–	–		
BMI	0.31	0.02	0.20	0.10		
Waist circumference (WC)	0.25	0.06	0.20	0.10		
Log-eVFA	0.30	0.02	0.27	0.02	0.54	0.37
Systolic blood pressure	−0.08	0.54	−0.09	0.44		
Diastolic blood pressure	0.20	0.14	−0.13	0.32		
Fasting glucose	0.05	0.69	0.03	0.82		
Hemoglobin A1c (JDS)	0.22	0.10	0.18	0.11		
HOMA-IR	0.33	0.06	0.29	0.04	0.03	5.10
AST	0.18	0.17	0.15	0.19		
ALT	0.29	0.03	0.16	0.18		
γ-GTP	−0.10	0.46	−0.06	0.59		
Total cholesterol	0.03	0.81	−0.08	0.52		
LDL-C	0.005	0.97	−0.09	0.42		
Triglyceride	0.32	0.02	0.19	0.12		
HDL-C	−0.30	0.02	−0.21	0.08		
Creatinine	−0.26	0.06	−0.18	0.22		
Log-adiponectin	−0.49	0.0001	−0.35	0.004	0.55	0.37
WBC	0.50	<0.0001	0.32	0.01	0.26	1.32
Neutrophilis	0.45	0.0003	0.32	0.008	–	–
Lymphocytes	0.43	0.0005	0.20	0.13		
Monocytes	0.36	0.0004	0.21	0.08		
Eosinophilis	0.28	0.03	0.18	0.14		
Basophilis	−0.08	0.55	−0.18	0.11		
CRP	0.39	0.003	0.35	0.001	0.21	1.65
Complication of DM	0.005	0.97	0.09	0.43		
Complication of HT	0.02	0.90	0.15	0.19		
Complication of DLP	0.14	0.30	0.02	0.88		
Mean IMT	−0.18	0.22	0.09	0.50		

Data are mean ± SD. BMI; body mass index, eVFA; estimated visceral fat area, HOMA-IR; homeostasis model assessment of insulin resistance, LDL-C; low density lipoprotein–cholesterol, HDL-C; high density lipoprotein–cholesterol, IMT; intima-media thickness.

Table 3
Correlation between peripheral blood S100A9 mRNA and clinical parameters.

Clinical parameters	Univariate (non-adjusted)		Univariate (age, sex-adjusted)		Multivariate	
	R	*P* value	*R*	*P* value	*P* value	*F* value
Age	−0.34	0.009	–	–		
Sex	0.04	0.75	–	–		
BMI	0.30	0.02	0.20	0.14		
Waist circumference (WC)	0.24	0.07	0.20	0.18		
Log-eVFA	0.26	0.05	0.23	0.06		
Systolic blood pressure	−0.24	0.08	−0.24	0.07		
Diastolic blood pressure	−0.05	0.73	−0.27	0.07		
Fasting glucose	0.06	0.64	0.05	0.72		
Hemoglobin A1c (JDS)	0.24	0.08	0.21	0.10		
HOMA-IR	0.33	0.06	0.30	0.07		
AST	0.14	0.31	0.11	0.41		
ALT	0.18	0.17	0.11	0.42		
γ-GTP	−0.18	0.20	−0.13	0.34		
Total cholesterol	−0.06	0.67	−0.14	0.29		
LDL-C	−0.04	0.78	−0.12	0.36		
Triglyceride	−0.18	0.20	0.14	0.30		
HDL-C	−0.32	0.02	−0.29	0.02	0.13	2.42
Creatinine	−0.31	0.02	−0.20	0.23		
Log-adiponectin	−0.31	0.02	−0.37	0.007	0.02	6.23
WBC	0.40	0.002	0.37	0.01	0.42	0.65
Neutrophilis	0.42	0.001	0.42	0.002	–	–
Lymphocytes	0.25	0.06	0.08	0.59		
Monocytes	0.29	0.03	0.21	0.11		
Eosinophilis	0.14	0.30	0.10	0.44		
Basophilis	−0.07	0.58	−0.17	0.20		
CRP	0.42	0.001	0.37	0.003	0.002	11.0
Complication of DM	0.06	0.67	0.12	0.35		
Complication of HT	0.06	0.71	0.07	0.61		
Complication of DLP	0.11	0.40	0.03	0.81		
Mean IMT	−0.19	0.19	−0.01	0.92		

Data are mean ± SD. BMI; body mass index, eVFA; estimated visceral fat area, HOMA-IR; homeostasis model assessment of insulin resistance, LDL-C; low density lipoprotein–cholesterol, HDL-C; high density lipoprotein–cholesterol, IMT; intima-media thickness.

Table 4
Correlation between peripheral blood S100A12 mRNA and clinical parameters.

Clinical parameters	Univariate (non-adjusted)		Univariate (age, sex-adjusted)		Multivariate	
	R	*P* value	*R*	*P* value	*P* value	*F* value
Age	−0.44	0.0006	–	–		
Sex	0.13	0.33	–	–		
BMI	0.38	0.004	0.31	0.02	–	–
Waist circumference (WC)	0.38	0.004	0.31	0.005	–	–
Log-eVFA	0.40	0.002	0.37	0.002	0.69	0.16
Systolic blood pressure	−0.09	0.51	−0.09	0.45		
Diastolic blood pressure	0.02	0.16	−0.05	0.72		
Fasting glucose	0.03	0.85	0.005	0.97		
Hemoglobin A1c (JDS)	0.20	0.14	0.17	0.17		
HOMA-IR	0.56	0.0008	0.52	0.0004	0.01	6.84
AST	0.19	0.16	0.16	0.19		
ALT	0.27	0.04	0.17	0.18		
γ-GTP	−0.12	0.39	−0.09	0.57		
Total cholesterol	−0.07	0.58	−0.16	0.19		
LDL-C	−0.07	0.62	−0.15	0.23		
Triglyceride	0.12	0.36	0.009	0.94		
HDL-C	−0.21	0.13	−0.13	0.31		
Creatinine	−0.20	0.15	−0.11	0.37		
Log-adiponectin	−0.40	0.002	−0.29	0.03	0.46	0.56
WBC	0.34	0.009	0.19	0.18		
Neutrophilis	0.30	0.02	0.19	0.15		
Lymphocytes	0.28	0.04	0.07	0.64		
Monocytes	0.22	0.11	0.09	0.50		
Eosinophilis	0.09	0.51	−0.01	0.94		
Basophilis	−0.07	0.59	−0.16	0.20		
CRP	0.44	0.0006	0.42	0.0005	0.06	3.88
Complication of DM	0.05	0.74	0.12	0.26		
Complication of HT	0.02	0.87	0.11	0.36		
Complication of DLP	0.04	0.79	0.07	0.63		
Mean IMT	−0.18	0.21	0.003	0.97		

Data are mean ± SD. BMI; body mass index, eVFA; estimated visceral fat area, HOMA-IR; homeostasis model assessment of insulin resistance, LDL-C; low density lipoprotein–cholesterol, HDL-C; high density lipoprotein–cholesterol, IMT; intima-media thickness.

Visceral fat accumulation causes dysregulation of adipocytokines and results in chronic low-grade inflammation in a whole body. There is a possibility that visceral fat-mediated inflammatory signal affects on peripheral blood cells and induces mRNA expressions of S100 family.

As shown in Table 2–4, HOMA-IR was directly associated with S100A8 ($F = 5.10$) and S100A12 ($F = 6.84$). Adiponectin ($F = 6.23$) and CRP ($F = 11.0$) were significant determinants of S100A9. These results suggest that S100A8, S100A9 and S100A12 in peripheral blood cells may be closely related to insulin resistance and inflammation in visceral fat accumulation.

The present study has several limitations. All subjects were inpatients and thus diabetes mellitus, dyslipidemia, and hypertension were common in the study population. These conditions could influence on the expression levels of various genes in peripheral blood cells directly or indirectly. In addition, the study participants were obese Japanese subjects (BMI $\geqslant$ 25 kg/m^2) and thus future studies are needed to perform among not only obese subjects but also non-obese healthy (low VFA) subjects.

Sources of funding

This work was supported by Grants-in-Aid for Scientific Research (C) No. 22590979 (to N. M.), Scientific Research on Innovative Areas No. 22126008 (to T. F.), and Takeda Science Foundation (to N. M.).

Disclosures

None.

Acknowledgments

We thank Miyuki Nakamura, Department of Metabolic Medicine, Graduate School of Medicine, Osaka University, for the excellent technical assistance.

Reference

[1] Y. Matsuzawa, Therapy insight: adipocytokines in metabolic syndrome and related cardiovascular disease, Nat. Clin. Pract. Cardiovasc. Med. 3 (2006) 35–42.
[2] O. Osborn, J.M. Olefsky, The cellular and signaling networks linking the immune system and metabolism in disease, Nat. Med. 18 (2012) 363–374.
[3] M.F. Gregor, G.S. Hotamisligil, Inflammatory mechanisms in obesity, Annu. Rev. Immunol. 29 (2011) 415–445.
[4] J.S. Flier, Obesity wars: molecular progress confronts an expanding epidemic, Cell 116 (2004) 337–350.
[5] M. Yamaoka, N. Maeda, S. Nakamura, S. Kashine, Y. Nakagawa, A. Hiuge-Shimizu, K. Okita, A. Imagawa, Y. Matsuzawa, K. Matsubara, T. Funahashi, I. Shimomura, A pilot investigation of visceral fat adiposity and gene expression profile in peripheral blood cells, PLoS ONE 7 (2012) e47377.
[6] M. Ryo, K. Maeda, T. Onda, M. Katashima, A. Okumiya, M. Nishida, T. Yamaguchi, T. Funahashi, Y. Matsuzawa, T. Nakamura, I. Shimomura, A new simple method for the measurement of visceral fat accumulation by bioelectrical impedance, Diabetes Care 28 (2005) 451–453.
[7] H. Nakatsuji, K. Kishida, T. Funahashi, M. Noguchi, T. Ogawa, Y. Okauchi, H. Nishizawa, T. Nakamura, Y. Matsuzawa, I. Shimomura, One -year reductions in body weight and blood pressure, but not in visceral fat accumulation and adiponectin, improve urinary albumin-to-creatinine ratio in middle-aged Japanese men, Diabetes Care 33 (2010) e110–e111.
[8] A. Hiuge-Shimizu, N. Maeda, A. Hirata, H. Nakatsuji, K. Nakamura, A. Okuno, S. Kihara, T. Funahashi, I. Shimomura, Dynamic changes of adiponectin and S100A8 levels by the selective peroxisome proliferator-activated receptor-gamma agonist rivoglitazone, Arterioscler. Thromb. Vasc. Biol. 31 (2011) 792–799.
[9] R Sekimoto, K Kishida, H Nakatsuji, T Nakagawa, T Funahashi, I Shimomura, High circulating levels of S100A8/A9 complex (calprotectin) in male Japanese with abdominal adiposity and dysregulated expression of S100A8 and S100A9

in adipose tissues of obese mice, Biochem. Biophys. Res. Commun. 419 (2012) 782–789.
[10] A. Hirata, K. Kishida, H. Nakatsuji, A. Hiuge-Shimizu, T. Funahashi, I. Shimomura, High serum S100A8/A9 levels and high cardiovascular complication rate in type 2 diabetic with ultrasonographic low carotid plaque density, Diabetes Res. Clin. Pract. 97 (2012) 82–90.
[11] A.M. Healy, M.D. Pickard, A.D. Pradhan, Y. Wang, Z. Chen, K. Croce, M. Sakuma, C. Shi, A.C. Zago, J. Garasic, A.I. Damokosh, T.L. Dowie, L. Poisson, J. Lillie, P. Libby, P.M. Ridker, D.I. Simon, Platelet expression profiling and clinical validation of myeloid-related protein-14 as a novel determinant of cardiovascular events, Circulation 113 (2006) 2278–2284.
[12] D.A. Morrow, Y. Wang, K. Croce, M. Sakuma, M.S. Sabatine, H. Gao, A.D. Pradhan, A.M. Healy, J. Buros, C.H. McCabe, P. Libby, C.P. Cannon, E. Braunwald, D.I. Simon, Myeloid-related protein 8/14 and the risk of cardiovascular death or myocardial infarction after an acute coronary syndrome in the Pravastatin or Atorvastatin evaluation and infection therapy: thrombolysis in myocardial infarction (PROVE IT-TIMI 22) trial, Am. Heart J. 155 (2008) 49–55.
[13] K. Croce, S100A8/A9 complex: more than just a biomarker of cardiovascular risk?, Circ J. 74 (2010) 626–627.
[14] O.H. Mortensen, A.R. Nielsen, C. Erikstrup, P. Plomgaard, C.P. Fischer, R. Krogh-Madsen, B. Lindegaard, A.M. Petersen, S. Taudorf, B.K. Pedersen, Calprotectin–a novel marker of obesity, PLoS ONE 4 (2009) e7419.
[15] V. Catalán, J. Gómez-Ambrosi, A. Rodríguez, B. Ramírez, F. Rotellar, V. Valentí, C. Silva, M.J. Gil, J.M. Fernández-Real, J. Salvador, G. Frühbeck, Increased levels of calprotectin in obesity are related to macrophage content: impact on inflammation and effect of weight loss, Mol. Med. 17 (2011) 1157–1167.
[16] S.Y. Lim, M.J. Raftery, J. Goyette, K. Hsu, C.L. Geczy, Oxidative modifications of S100 proteins: functional regulation by redox, J. Leukoc. Biol. 86 (2009) 577–587.
[17] T. Vogl, K. Tenbrock, S. Ludwig, N. Leukert, C. Ehrhardt, M.A. van Zoelen, W. Nacken, D. Foell, T. van der Poll, C. Sorg, J. Roth, Mrp8 and Mrp14 are endogenous activators of toll-like receptor 4, promoting lethal, endotoxin-induced shock, Nat. Med. 13 (2007) 1042–1049.
[18] E. Leclerc, G. Fritz, S.W. Vetter, C.W. Heizmann, Binding of S100 proteins to RAGE: an update, Biochim. Biophys. Acta 1793 (2009) 993–1007.
[19] A. Kosaki, T. Hasegawa, T. Kimura, K. Iida, J. Hitomi, H. Matsubara, Y. Mori, M. Okigaki, N. Toyoda, H. Masaki, M. Inoue-Shibata, M. Nishikawa, T. Iwasaka, Increased plasma S100A12 (EN-RAGE) levels in patients with type 2 diabetes, J. Clin. Endocrinol. Metab. 89 (2004) 5423–5428.
[20] G. Basta, A.M. Sironi, G. Lazzerini, S. Del Turco, E. Buzzigoli, A. Casolaro, A. Natali, E. Ferrannini, A. Gastaldelli, Circulating soluble receptor for advanced glycation end products is inversely associated with glycemic control and S100A12 protein, J. Clin. Endocrinol. Metab. 91 (2006) 4628–4634.
[21] Y. Mori, A. Kosaki, N. Kishimoto, T. Kimura, K. Iida, M. Fukui, F. Nakajima, M. Nagahara, M. Urakami, T. Iwasaka, H. Matsubara, Increased plasma S100A12 (EN-RAGE) levels in hemodialysis patients with atherosclerosis, Am. J. Nephrol. 29 (2009) 18–24.
[22] J. Gawdzik, L. Mathew, G. Kim, T.S. Puri, M.A. Hofmann Bowman, Vascular remodeling and arterial calcification are directly mediated by S100A12 (EN-RAGE) in chronic kidney disease, Am. J. Nephrol. 33 (2011) 250–259.
[23] T. Ebihara, R. Endo, H. Kikuta, N. Ishiguro, X. Ma, M. Shimazu, T. Otoguro, K. Kobayashi, Differential gene expression of S100 protein family in leukocytes from patients with Kawasaki disease, Eur. J. Pediatr. 164 (2005) 427–431.
[24] N. Mahajan, N. Malik, A. Bahl, V. Dhawan, Receptor for advanced glycation end products (RAGE) and its inflammatory ligand EN-RAGE in non-diabetic subjects with pre-mature coronary artery disease, Atherosclerosis 207 (2009) 597–602.